Beryllium Compounds

Deutsche Ausgabe: DOI: 10.1002/ange.201606154
Internationale Ausgabe: DOI: 10.1002/anie.201606154

The Oxygen-Rich Beryllium Oxides BeO_4 and BeO_6

Qingnan Zhang, Paul Jerabek, Mohua Chen, Mingfei Zhou, and Gernot Frenking**

Abstract: *Two novel isomers of BeO_4 with the structures OBeOOO and OBe(O_3) in the electronic triplet state have been prepared as well as the known disuperoxide complex Be(O_2)$_2$ in solid noble-gas matrices. We also report the synthesis of the oxygen-rich bis(ozonide) complex Be(O_3)$_2$ in the triplet state which has a D_{2d} equilibrium geometry. The molecular structures were identified by infrared absorption spectroscopy with isotopic substitutions as well as quantum chemical calculations.*

Although beryllium resides in the same row as boron, nitrogen, carbon, and oxygen in the periodic table, the chemistry of beryllium has remained sketchy so far compared with that of the other elements of the first octal row of the periodic system. This is probably due to the high toxicity of beryllium compounds, which prevented large-scale experimental work for a long time, with notable exceptions.[1] Recent work indicates that beryllium chemistry may now become the focus of more intensive experimental studies.[2]

The structure and bonding of beryllium compounds are of significant experimental and theoretical interest. Owing to its high ionization energy and small atomic radius, covalent interactions play an important role in the bonding in many beryllium compounds, unlike the heavier alkaline-earth metals Mg–Ba.[3] Beryllium oxide species have gained experimental and theoretical attention, because of their unique bonding situation. The simplest beryllium oxide, BeO was characterized to be the strongest diatomic Lewis acid, which was found to be able to bind a noble gas atom in forming the complexes NgBeO (Ng = He–Xe).[4,5] The beryllium dioxide molecule BeO_2 has been prepared in solid noble-gas matrices and was characterized to be a linear molecule with a triplet ground state.[6–8] The less stable cyclic Be(O_2) isomer can also be stabilized by argon coordination as ArBe(O_2) complex in a solid argon matrix.[7] The hyperstoichiometric BeOBe and the cation $BeOBe^+$ were spectroscopically determined to have very similar linear centrosymmetric structures.[6,9–12] Higher beryllium oxide species have also been reported in solid noble-gas matrices. The Be(O_2)$_2$ complex is characterized to be a disuperoxide with a D_{2d} structure.[6,7] The cyclic Be_2O_2 and two Be_2O_4 isomers have also been prepared and spectroscopically identified.[6,13] Herein we provide a joint matrix-isolation infrared spectroscopic and theoretical study on some novel oxygen-rich beryllium–oxygen species. Two additional structural isomers of the previously reported disuperoxide Be(O_2)$_2$ complex involving an end-on and a side-on bonded ozonide fragment, respectively, and a bis(ozonide) complex Be(O_3)$_2$ were synthesized and identified.

The beryllium–oxygen species were prepared by the reactions of beryllium atoms and dioxygen molecules in solid argon, and were detected by infrared absorption spectroscopy as described in detail previously.[14] The infrared spectra in the 1450–750 cm^{-1} region from co-deposition of Be atoms with 0.3 % O_2 in argon are shown in Figure 1. After 1 h of sample deposition at 4 K (Figure 1, trace a), absorptions at 1413.4, 1118.7, 988.6, and 953.8 cm^{-1} were observed. The 1118.7 and 953.8 cm^{-1} absorptions are due to the O_4^+ cation and O_4^- anion, which are common for laser-evaporated metal-atom reactions with dioxygen.[15,16] The 1413.4 and 988.6 cm^{-1} absorptions were previously assigned to the antisymmetric stretching vibrations of the linear OBeO and $OBeO^+$ species, respectively.[6,7] When the as-deposited sample was subjected to broad band irradiation using a mercury arc lamp without a filter ($250 < \lambda < 580$ nm); Figure 1, trace b), the charged species absorptions were completely destroyed, while the OBeO absorption increased

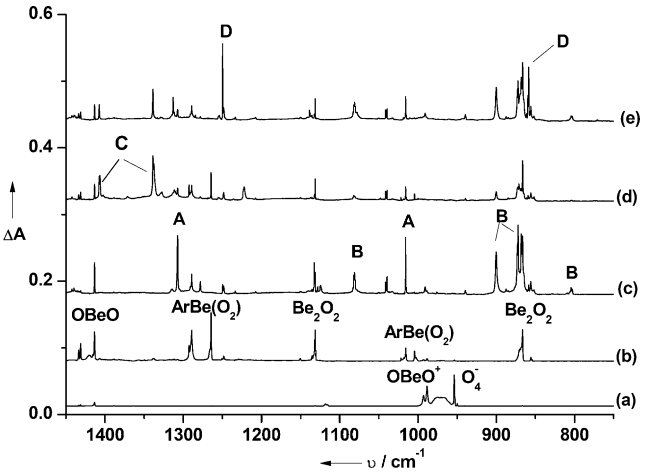

Figure 1. Infrared spectra in the 1450–750 cm^{-1} region from co-deposition of Be atoms with 0.3 % O_2 in argon. a) after 1 h of sample deposition at 4 K, b) after 30 min of UV/Vis light irradiation (250–580 nm), c) after annealing to 30 K, d) after 15 min of UV/Vis light irradiation, and e) after annealing to 25 K. **A**: Be(O_2)$_2$, **B**: Be(O_3)$_2$, **C**: OBeOOO, and **D**: OBe(O_3).

[*] Q. Zhang, Prof. M. Chen, Prof. M. Zhou
Collaborative Innovation Center of Chemistry for Energy Materials, Department of Chemistry, Shanghai Key Laboratory of Molecular Catalysts and Innovative Materials, Fudan University
Shanghai 200433 (China)
E-mail: mfzhou@fudan.edu.cn
Dr. P. Jerabek, Prof. G. Frenking
Fachbereich Chemie
Philipps-Universität Marburg
Hans-Meerwein-Strasse, 35043 Marburg (Germany)
E-mail: frenking@chemie.uni-marburg.de

Supporting information for this article can be found under: http://dx.doi.org/10.1002/anie.201606154.

markedly along with the formation of cyclic Be_2O_2 (1131.3, 866.3, and 522.4 cm^{-1}) and $ArBe(O_2)$ (1289.1/1264.3 and 1015.6/1004.4 cm^{-1}).[6] Subsequent sample annealing to 30 K (Figure 1, trace c) produced two groups of new absorptions (labeled as **A** and **B**) at the expense of the OBeO and $ArBe(O_2)$ absorptions. Both group **A** and **B** absorptions were almost destroyed on additional broad band UV/Vis irradiation (Figure 1, trace d) during which a new species **C** was produced. Group **C** absorptions disappeared on following sample annealing to 25 K (Figure 1, trace e), while a new species **D** was produced and species **B** was partially recovered. The experiments were repeated under the same conditions using the $^{18}O_2$, $^{16}O_2+{}^{18}O_2$, and $^{16}O_2+{}^{16}O^{18}O+{}^{18}O_2$ samples to help product identification on the basis of isotopic shifts and absorption splittings. The isotopic spectra in selected regions are shown in Figures S1–S4 of the Supporting Information. The product band positions are summarized in Table 1.

Experiments were also performed with laser-evaporated beryllium atoms and O_2 in excess neon. The spectra with a 0.03 % O_2 in neon are shown in Figure 2. The same products as observed in the argon matrix are presented, but the product absorptions are much weaker than those observed in the argon matrix, particularly for the BeO_4 isomers. The product absorptions in solid neon are given in parentheses in Table 1. The band positions are uniformly shifted to higher wave numbers from those of in solid argon.

Species **A** with absorptions at 1307.0, 1015.8, and 596.4 cm^{-1} in solid argon is assigned to the beryllium disuperoxide complex $Be(O_2)_2$ with D_{2d} symmetry. The first

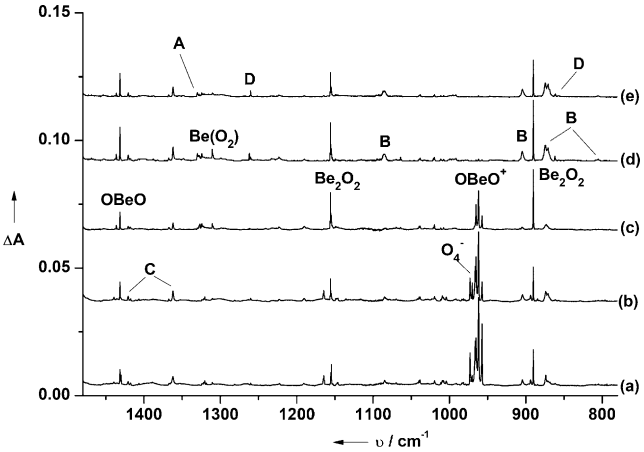

Figure 2. Infrared spectra in the 1480–780 cm^{-1} region from co-deposition of laser-evaporated Be atoms with 0.03 % O_2 in neon. a) 30 min sample deposition at 4 K, b) after annealing to 10 K, c) after 15 min of 280–580 nm light irradiation, d) after 15 min of 250–580 nm light irradiation, and e) after 12 K annealing. **A**: $Be(O_2)_2$, **B**: $Be(O_3)_2$, **C**: OBeOOO, and **D**: $OBe(O_3)$.

absorption was attributed to this species previously.[7] The mixed isotopic spectral features (Figure S1 and S2, Table S1) confirm that two equivalent O_2 units with equivalent oxygen atoms are involved. The band position and isotopic frequency ratio (1.0472) suggest that the 1015.8 cm^{-1} absorption is mainly an antisymmetric O–O stretching vibration. The 596.4 cm^{-1} absorption can be attributed to the antisymmetric OBeO stretching mode, which is doubly degenerate for the

Table 1: Experimental and calculated infrared absorptions and isotope shifts (Δ, cm^{-1}) of the BeO_4 and BeO_6 compounds.

Species	Exptl.[d]			Assignment	Calcd. CCSD/cc-pVTZ[c]			M06-2X/def2-TZVPP		
	$^{16}O_2$	$^{18}O_2$	Δ		$^{16}O_2$	$^{18}O_2$	Δ	$^{16}O_2$	$^{18}O_2$	Δ
$Be(O_2)_2$ (**A**)	1307.0 (1330.1)	1282.8 (1311.0)	−24.2 (−19.1)	Be-O,O-O s-str[e]	1320.3	1297.7	−22.6	1362.3	1329.6	−32.7
	1015.8	970.0	−45.8	Be-O,O-O a-str[e]	1126.1	1072.6	−53.5	1194.6	1145.9	−48.7
	596.4	578.6	−17.8	O-Be-O a-str	619.0[a]	600.6	−19.0	648.5[a]	627.2	−21.3
$OBe(O_3)$ (**D**)	1249.5 (1262.0)	1230.1 (1242.2)	−19.4 (−19.8)	Be-O str	1298.9	1281.6	−17.3	1312.7	1293.7	−19.0
	858.6 (861.8)	816.2 (818.7)	−42.4 (−43.1)	O-O-O a-str	932.2	888.3	−43.9	997.0	946.6	−50.4
OBeOOO (**C**)	1407.4 (1420.7)	1380.9 (1392.1)	−26.5 (−28.6)	O-O, O-Be-O str	1421.5	1402.2	−19.3	1460.1	1437.6	−22.5
	1338.7 (1362.0)	1272.4 (1296.9)	−66.3 (−65.1)	O-O, O-Be-O str	1258.9	1188.0	−70.9	1342.6	1269.5	−73.1
	497.8	473.8	−24.0	O-O str	472.4	446.7	−25.7	468.2	442.8	−25.4
Ar-OBeOOO				O-Be-O str				1472.3	1450.8	−21.5
				O-O str				1340.6	1266.7	−73.9
				O-O str				470.3	444.7	−25.6
OBeOOO-Ar				O-Be-O str				1458.0	1435.7	−22.3
				O-O str				1341.1	1268.0	−73.1
				O-O str				475.6	449.6	−26.0
$Be(O_3)_2$ (**B**)	1080.8 (1085.5)	1050.7 (1055.6)	−30.1 (−29.9)	Be-O,O-O str	1138.2	1089.9	−48.3	1204.6	1142.8	−61.8
	900.2 (904.5)	881.8 (886.1)	−18.4 (−18.4)	Be-O str	1000.4	976.3	−24.1	1009.0	993.7	−15.3
	872.1 (874.5)	829.4 (832.2)	−42.7 (−42.3)	O-O-O a-str	936.5[a]	892.8[a]	−44.7	1004.5	953.3	−51.2
	804.4 (805.2)	776.9 (777.3)	−27.5 (−27.9)	O-O-O bend	786.0[b]	767.2[b]	−18.8	815.1[b]	771.6[b]	−43.5

[a] Average value of two nearby lying signals; [b] Very low intensity; [c] The values for OBeOOO were calculated at CCSD/aug-cc-pVTZ; [d] Experimental values in solid argon. The data in parentheses were obtained in solid neon; [e] s-str: symmetric stretch; a-str: asymmetric stretch.

D_{2d} symmetry molecule. Only one weak band at 1330.1 cm^{-1} is observed in solid neon for $Be(O_2)_2$.

Species **C** with absorptions at 1407.4, 1338.7, and 497.8 cm^{-1} in solid argon is attributed to the OBeOOO molecule, a structural isomer of $Be(O_2)_2$. Details on the spectral assignment of the experimentally observed modes are provided in Supporting Information. They agree with the assignments that come from the calculated spectra. The band position and isotopic $^{16}O/^{18}O$ ratio (1.0192) suggest that the upper mode is mainly an antisymmetric OBeO stretching vibration. The middle mode has an isotopic $^{16}O/^{18}O$ ratio of 1.0521, which is largely due to an O–O stretching vibration. The low frequency mode also shows quite large isotopic $^{16}O/^{18}O$ ratio (1.0507), and is attributed to the stretching vibration of the weak OBeO–OO bond. Similar complexes involving a bent OOO unit have been reported for some transition- and main-group-metal systems with comparable O–O stretching frequencies.[13,17,18] The OBeOOO molecule in solid neon is observed at 1420.7 and 1362.0 cm^{-1}. The band positions are 13.3 and 23.3 cm^{-1} blue-shifted from argon to neon.

Species **D** with absorptions at 1249.5 and 858.6 cm^{-1} in solid argon is attributed to the $OBe(O_3)$ molecule, a third structural isomer with BeO_4 stoichiometry. This species is interconvertible with the OBeOOO isomer. The isotopic frequency ratio (1.0158) and mixed isotopic spectral features (Figure S4) are consistent with the assignment of the 1249.5 cm^{-1} absorption to the terminal Be–O stretching vibration that is coupled by a side-on bonded O_3 unit. The low absorption with an isotopic $^{16}O/^{18}O$ ratio of 1.0519 is appropriate for the antisymmetric stretching vibration of the O_3 subunit. Side-on bonded ozonide complexes have been reported for a number of early transition-metal and main-group-metal systems.[14,17–20] The same molecule absorbs at 1262.0 and 861.8 cm^{-1} in solid neon, which are only 12.5 and 3.2 cm^{-1} blue-shifted from those of in argon, suggesting weak matrix effect.

Four absorptions were observed for species **B** at 1080.8, 900.2, 872.1, and 804.4 cm^{-1} in solid argon. These absorptions are favored with relatively high O_2 concentrations, and show strong correlation with the OBeO absorption (The spectra with the 0.2% and 0.1% O_2 samples are shown in Figure S5 and S6). The isotopic spectral features imply the assignment of species **B** to $Be(O_3)_2$ with D_{2d} symmetry formed by the reaction of OBeO with two dioxygen molecules (See Supporting Information for details). The absorption at 872.1 cm^{-1} shifted to 829.4 cm^{-1} with $^{18}O_2$. The $^{16}O/^{18}O$ isotopic frequency ratio of 1.0515 indicates that it is mainly due to an O–O stretching vibration. The band position and isotopic data point to the assignment of this absorption to the doubly degenerate antisymmetric O_3 stretching vibration. The 900.2 cm^{-1} absorption shifted to 881.8 cm^{-1} with $^{18}O_2$. The $^{16}O/^{18}O$ isotopic frequency ratio (1.0209) implies that this absorption is largely due to a Be–O stretching mode. The 1080.8 cm^{-1} absorption has an ^{18}O counterpart at 1050.7 cm^{-1}. The $^{16}O/^{18}O$ isotopic frequency ratio of 1.0286 is higher than those of any Be–O stretching modes but is much lower than that of O–O stretching vibration, which implies that this absorption is due to a mixed mode of Be–O stretching and O–O stretching vibrations. The very weak absorption at 804.4 cm^{-1} is likely due to a O_3 bending vibration. The $Be(O_3)_2$ complex is observed at 1085.5, 904.5, 874.5, and 805.2 cm^{-1} in solid neon. The band positions are blue-shifted less than 5 cm^{-1} from those in solid argon.

We carried out quantum chemical calculations of the molecules $Be(O_2)_2$, OBeOOO, $OBe(O_3)$, and $Be(O_3)_2$ using ab initio methods at the CCSD/cc-pVTZ level and density functional theory (DFT) at M06-2X/def2-TZVPP. Details of the methods are given in Supporting Information. Calculated data in this work refer to CCSD/cc-pVTZ calculations, unless otherwise marked. Calculations of the four species at the singlet and triplet electronic state showed that the triplets are always much lower in energy than the singlets. Figure 3 display the optimized geometries. The most stable isomer on the BeO_4 potential energy surface is the disuperoxide $Be(O_2)_2$ with D_{2d} symmetry (Figure 3, structure (a)) which agrees with earlier work.[6,7] The oxo-ozonide isomer $OBe(O_3)$, which has a cyclic BeO_3 moiety and C_{2v} symmetry (structure (b)), is at the CCSD/cc-pVTZ level 28.2 kcal mol^{-1} higher in energy than $Be(O_2)_2$ (28.1 kcal mol^{-1} at M06-2X/def2-TZVPP). The calculated reaction energies that are shown in Table 2 suggest

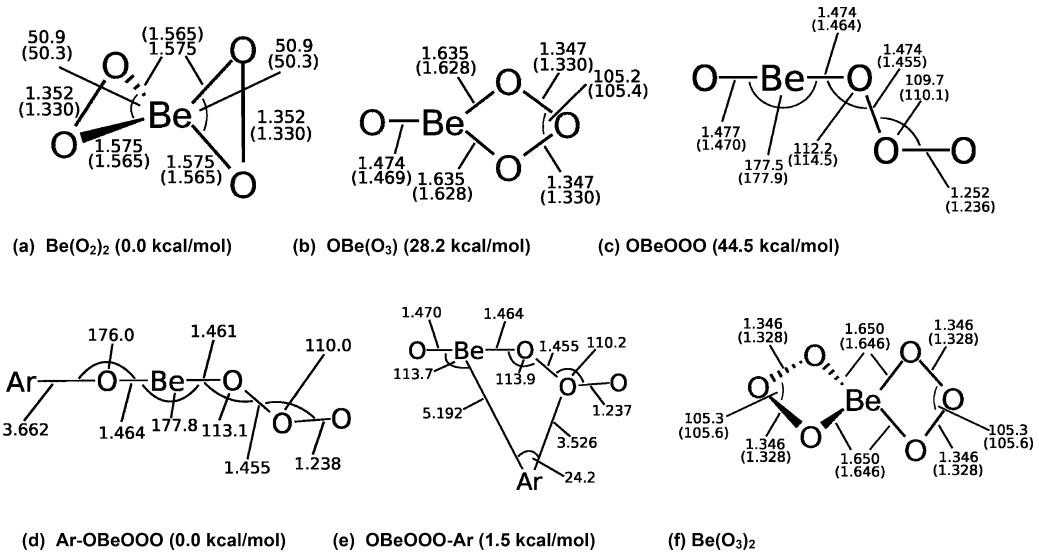

Figure 3. Optimized geometries and relative energies of the beryllium oxides at the CCSD/cc-pVTZ level (CCSD/aug-cc-pVTZ for OBeOOO). Bond lengths [Å], angles [°]. Values at M06-2X/def2-TZVPP are given in parentheses. Geometries and relative energies of Ar-OBeOOO and OBeOOO-Ar are optimized at M06-2X/def2-TZVPP. All species have an electronic triplet state.

Table 2: Calculated reaction energies for oxidation of Be and BeO in kcal mol^{-1} at CCSD/cc-pVTZ.[a]

BeO_n	$Be + n/2\,O_2 \rightarrow BeO_n$	$BeO + (n\text{-}1)/2\,O_2 \rightarrow BeO_n$
BeO	−36.6 (−35.5)	
$Be(O_2)_2$	−123.1 (−119.2)	−86.5 (−83.7)
O-Be-OOO	−91.4 (−88.1)	−54.8 (−52.6)
O-Be-(O_3)	−94.9 (−91.1)	−58.3 (−55.6)
$Be(O_3)_2$	−104.9 (−99.1)	−68.3 (−63.5)

[a] The values in parentheses include zero-point vibrational corrections.

that all beryllium oxides $Be(O_2)_2$, OBeOOO, $OBe(O_3)$, and $Be(O_3)_2$ are thermodynamically stable for dissociation into $BeO + O_2$ and total loss of oxygen. However, the bis(ozonide) $Be(O_3)_2$ is thermodynamically unstable towards loss of O_2 and formation of $Be(O_2)_2$. Note that the difference between the first and second columns give the stability for the reaction $Be + 0.5\,O_2 \rightarrow X(^1\Sigma^+)$ BeO which is shown in the first entry line. The dissociation of BeO_2 in the lowest lying $^3\Sigma_g^-$ ground state into $Be + O_2$ has been calculated before.[8b] The theoretical value of 88 ± 4 kcal mol^{-1} indicates that $Be(O_2)_2$, which has a calculated bond dissociation energy (BDE) for loss of O_2 of BDE = 123.1 kcal mol^{-1}, is thermodynamically the most stable beryllium oxide of the BeO_x species.

The planar acyclic oxo-ozonide OBeOOO (C_s symmetry, Figure 3, structure (c)) was found as stationary point at the M06-2X/def2-TZVPP level and 45.8 kcal mol^{-1} higher in energy than $Be(O_2)_2$, Optimization at CCSD/cc-pVTZ did not succeed, but augmentation of the basis set with diffuse functions at the CCSD/aug-cc-pVTZ level gave a stationary point, which is 44.5 kcal mol^{-1} higher in energy than $Be(O_2)_2$ using a single-point energy of the $Be(O_2)_2$ isomers at CCSD/cc-pVTZ//CCSD/aug-cc-pVTZ. The frequency calculations of the optimized structures of OBeOOO at CCSD/aug-cc-pVTZ and M06-2X/def2-TZVPP gave a small imaginary mode at both levels of theory. We optimized the geometry of OBeOOO at the M06-2X/def2-TZVPP level with one attached Ar atom and found two energy minima denoted as Ar-OBeOOO and OBeOOO-Ar with nearly the same energy (Figure 3, structures (d) and (e)) which exhibit slightly distorted geometries of the OBeOOO moiety. The oxygen-rich bis(ozonide) $Be(O_3)_2$ exhibits a D_{2d} structure with perpendicular O_3 moieties (Figure 3, structure (f)). The bond lengths and angles of the BeO_3 fragments in the bis(ozonide) $Be(O_3)_2$ are very similar to the values of the cyclic ozonide fragment in $OBe(O_3)$. The theoretical bond lengths and angles at M06-2X/def2-TZVPP agree quite well with the CCSD/cc-pVTZ data.

The assignment of the vibrational spectra and the identification of the observed species was made by comparing the experimental signals with the calculated harmonic frequencies and the oxygen isotope shifts Δ ($\nu^{16}O - \nu^{18}O$) which are shown in Table 1. It is well established that the calculated harmonic frequencies are in general, higher than the experimental anharmonic frequencies. The noble-gas matrix effect, which is not considered by the calculations, is another factor that contributes to the difference between the matrix experimental and computed values. Table 1 shows that the isotopic shifts of the three observed IR modes for species **A** agree very well with the calculated data of the global energy minimum structure $Be(O_2)_2$ at both levels of theory. The absolute values of the calculated frequencies at CCSD/cc-pVTZ are slightly too high with the M06-2X/def2-TZVPP values being even higher. The newly discovered isomer $OBe(O_3)$ is also easily identified by comparing the experimental signals for species **D** with the calculated frequencies and isotope shifts Δ of the two signals (Table 1). The identification of species **B** as oxygen rich BeO_6 is also straightforward. Table 1 shows that the calculated frequencies agree very well with the experimental data.

The identification of the energetically rather high lying isomer OBeOOO as species **C** was more difficult. As mentioned above, the optimized structures at M06-2X/def2-TZVPP and CCSD/aug-cc-pVTZ have one small imaginary frequency (Table S3). The vibrational frequencies of the complexes Ar-OBeOOO and OBeOOO-Ar which are genuine energy minima are only lightly different from the values for free OBeOOO. Table 1 shows that the three experimentally observed modes and the isotope shifts of species **C** agree very well with the calculated frequencies of OBeOOO, Ar-OBeOOO, and OBeOOO-Ar. We think that the weak interactions of the surrounding noble-gas atoms stabilize the OBeOOO-Ar isomer such that it becomes an observable species.

In summary, the novel oxygen-rich species BeO_6 and three isomers of BeO_4 with the structures $(O_2)Be(O_2)$, OBeOOO, and $OBe(O_3)$ have been synthesized via the reactions of beryllium atoms with dioxygen molecules in solid argon and neon. The matrix-isolation infrared spectroscopy in conjunction with isotopic substitution provides unequivocal evidence about the number of oxygen atoms contained in the species as well as the binding mode and oxidation state. The species characterized herein, together with the previously known BeO_2 molecule, demonstrate diverse bonding situations between beryllium and oxygen. All these complexes are identified to have electronic triplet ground states with the beryllium center in its most common oxidation state + II and up to six oxygen atoms can bind to one beryllium center in different oxidation states, that is, oxyl radical $(O)^-$, superoxide $(O_2)^-$, and ozonide $(O_3)^-$.

Acknowledgements

The work at Fudan was financially supported by the National Natural Science Foundation (Grant No. 21433005), Ministry of Science and Technology of China (2013CB834603).

Keywords: beryllium oxides · matrix isolation · ozonide complexes · quantum chemical calculations

How to cite: *Angew. Chem. Int. Ed.* **2016**, *55*, 10863–10867
Angew. Chem. **2016**, *128*, 11021–11025

[1] Systematic experimental studies about structure and reactivity of beryllium compounds have been reported by Dehnicke and co-workers in more than 40 publications (mostly written in German) since 2003. Representative examples are: a) B. Neu-

müller, F. Weller, K. Dehnicke, *Z. Anorg. Allg. Chem.* **2003**, *629*, 2195; b) W. Massa, K. Dehnicke, *Z. Anorg. Allg. Chem.* **2007**, *633*, 1366; c) R. Tonner, G. Frenking, B. Neumüller, K. Dehnicke, *Z. Anorg. Allg. Chem.* **2007**, *633*, 1183; d) B. Neumüller, K. Dehnicke, R. Puchta, *Z. Anorg. Allg. Chem.* **2008**, *634*, 1473; e) G. Frenking, N. Holzmann, B. Neumüller, K. Dehnicke, *Z. Anorg. Allg. Chem.* **2010**, *636*, 1772; f) W. Petz, K. Dehnicke, N. Holzmann, G. Frenking, B. Neumüller, *Z. Anorg. Allg. Chem.* **2011**, *637*, 1702; g) K. Dehnicke, B. Neumüller, *Z. Anorg. Allg. Chem.* **2008**, *634*, 2703.

[2] M. Arrowsmith, H. Braunschweig, M. A. Celik, T. Dellermann, R. D. Dewhurst, W. C. Ewing, K. Hammond, T. Kramer, I. Krummenacher, J. Mies, K. Radacki, J. K. Schuster, *Nat. Chem.* **2016**, DOI: 10.1038/nchem.2542; For a theoretical study see: S. A. Couchman, N. Holzmann, G. Frenking, D. J. D. Wilson, J. L. Dutton, *J. Chem. Soc. Dalton Trans.* **2013**, *42*, 11375; D. Naglav, M. Buchner, G. Bendt, F. Kraus, S. Schulz, *Angew. Chem. Int. Ed.* **2016**, *55* DOI: 10.1002/anie.201601809; *Angew. Chem.* **2016**, *128*, DOI: 10.1002/ange.201601809; M. H. Chen, Q. N. Zhang, M. F. Zhou, D. M. Andrada, G. Frenking, *Angew. Chem.* **2015**, *127*, 126; *Angew. Chem. Int. Ed.* **2015**, *54*, 124.

[3] M. C. Heaven, V. E. Bondybey, J. M. Merritt, A. L. Kaledin, *Chem. Phys. Lett.* **2011**, *506*, 1.

[4] a) W. Koch, J. R. Collins, G. Frenking, *Chem. Phys. Lett.* **1986**, *132*, 330; b) G. Frenking, W. Koch, J. Gauss, D. Cremer, *J. Am. Chem. Soc.* **1988**, *110*, 8007; c) G. Frenking, W. Koch, F. Reichel, D. Cremer, *J. Am. Chem. Soc.* **1990**, *112*, 4240; d) A. Veldkamp, G. Frenking, *Chem. Phys. Lett.* **1994**, *226*, 11.

[5] C. A. Thompson, L. Andrews, *J. Am. Chem. Soc.* **1994**, *116*, 423.

[6] C. A. Thompson, L. Andrews, *J. Chem. Phys.* **1994**, *100*, 8689.

[7] L. Andrews, G. V. Chertihin, C. A. Thompson, J. Dillon, S. Byrne, C. W. Bauschlicher, Jr., *J. Phys. Chem.* **1996**, *100*, 10088.

[8] a) T. J. Lee, R. Kobayashi, N. C. Handy, R. D. Amos, *J. Chem. Phys.* **1992**, *96*, 8931; b) C. W. Bauschlicher, Jr., H. Partridge, M. Sodupe, S. R. Langhoff, *J. Phys. Chem.* **1992**, *96*, 9259.

[9] L. P. Theard, D. L. Hildenbrand, *J. Chem. Phys.* **1964**, *41*, 3416.

[10] J. M. Merritt, V. E. Bondybey, M. C. Heaven, *J. Phys. Chem. A* **2009**, *113*, 13300.

[11] B. Ostojic, P. Jensen, P. Schwerdtfeger, B. Assadollahzadeh, P. R. Bunker, *J. Mol. Spectrosc.* **2010**, *263*, 21.

[12] I. O. Antonov, B. J. Barker, M. C. Heaven, *J. Chem. Phys.* **2011**, *134*, 044306.

[13] Z. J. Zhou, Y. Z. Li, J. Zhuang, G. J. Wang, M. H. Chen, Y. Y. Zhao, X. M. Zheng, M. F. Zhou, *J. Phys. Chem. A* **2011**, *115*, 9947.

[14] a) M. F. Zhou, L. Andrews, C. W. Bauschlicher, Jr., *Chem. Rev.* **2001**, *101*, 1931; b) G. J. Wang, M. F. Zhou, *Int. Rev. Phys. Chem.* **2008**, *27*, 1.

[15] G. V. Chertihin, L. Andrews, *J. Chem. Phys.* **1998**, *108*, 6404.

[16] M. F. Zhou, J. Hacaloglu, L. Andrews, *J. Chem. Phys.* **1999**, *110*, 9450.

[17] C. X. Wang, M. H. Chen, Z. H. Li, M. F. Zhou, *J. Phys. Chem. A* **2013**, *117*, 11217.

[18] Y. Gong, M. F. Zhou, S. X. Tian, J. L. Yang, *J. Phys. Chem. A* **2007**, *111*, 6127.

[19] a) Y. Gong, C. F. Ding, M. F. Zhou, *J. Phys. Chem. A* **2007**, *111*, 11572; b) Y. Gong, C. F. Ding, M. F. Zhou, *J. Phys. Chem. A* **2009**, *113*, 8569.

[20] a) Y. Gong, M. F. Zhou, *J. Phys. Chem. A* **2008**, *112*, 9758; b) Y. Gong, M. F. Zhou, *J. Phys. Chem. A* **2007**, *111*, 8973.

Received: June 24, 2016
Published online: August 5, 2016

